Novel Navigation Strategy Study on Autonomous Mobile Robots

Peng Jia pengjia_sdut@126.com
Ph.D Candidate/ School of Mechanical and Precision Instrument Engineering, Xi'an University of Technology Xi'an, 710048, China College of Computer Science and Technologe Shandong University of Technology Zibo, 255049, China

Yumei Huang hym_xaut@126.com
Faculty/School of Mechanical and Precision Instrument Engineering, Xi'an University of Technology Xi'an, 710048, China

Feng Gao gf2713@xaut.edu.cn
Faculty/School of Mechanical and Precision Instrument Engineering, Xi'an University of Technology Xi'an, 710048, China

Yan Li liyangf@xaut.edu.cn
Faculty/School of Mechanical and Precision Instrument Engineering, Xi'an University of Technology Xi'an, 710048, China

Abstract

Potential field method has been widely used in obstacle avoidance for mobile robots because of its elegance and simplicity. However, this method has inherent drawbacks. Considering this, this paper introduces a new behaviour-based navigation strategy. Aiming at a mobile robot SDLG-1 developed by the authors, the kinematics model is built based on its motion structure. Using twelve sonar sensors, the strategy algorithm of behaviour-based navigation control is brought forth. Based on the algorithm, software simulations and experimental evaluations have been conducted. Both results indicate the navigation strategy proposed in this paper is effective.

Keywords: Behaviour-based navigation, mobile robot, kinematics model

1. INTRODUCTION

The task of navigation is to plan a path to a specified goal and to execute this plan, modifying it as necessary to avoid unexpected obstacles. Intelligent navigation of mobile robot is one of the challenging tasks among the researches and scientists throughout the world [1]. Potential field method (PFM) for obstacle avoidance has become popular among researches in the filed of robots and mobile robots. The idea of imaginary forces acting on a robot has been suggested by Andrews and Khatib [2, 3]. In the approach, obstacles exert repulsive forces onto the robot while the target applies an attractive force to the robot. The sum of all forces determines the subsequent orientation and speed of travel. The main reason for the popularity of PFM is its

simplicity and elegance. Simple PFM can be implemented quickly and initially provide acceptable results without requiring many refinements [4]. In [5], the PFM is applied to off-line planning for robot navigations. Literature [6] proposed a generalized PFM to combine global and local path planning. The PFM has been implemented on mobile robots with real sensory data in [7, 8]. However, the mobile robot is very slow to avoid obstacles at 1.2mm/sec. In [9], a PFM called virtual force field (VFF) has been developed. Based on the VFF experiment and research, four defects of potential field method have been found: (1) trap situations exist due to local minima; (2) no passage between closely spaced obstacles; (3) oscillations in the presence of obstacles; (4) oscillation in narrow passages [4]. Although PFM has been updated in the following researches [10-12], the four principle defects still possibly affect the final navigation results. Considering the defects of potential field method, a behaviour-based navigation control algorithm is introduced in this paper. Evaluations by software simulations have been successfully conducted on the indoor autonomous mobile robot SDLG-1 developed by the authors.

2. KINEMATICS MODEL OF SDLG-1

2.1 Motion structure of the SDLG-1

The mobile robot SDLG-1 has two drive wheels and two passive wheels. Two-wheeled differential drive system is applied in the design of the mobile robot SDLG-1 as shown in Figure 1. The driving wheel system is composed of brushless DC servo motor, photoelectric rotary encoder, hub of axle-coding wheel and hub of driving wheel. Relative positions of the robot can be realized referring the photoelectric encoder and its wheel hub by the voyage method [13]. The symbols used in Figure 1 are listed and explained as follows.

ov is the center between the two drive wheels. l is the distance between the two drive wheels. ϕ is the orientation angle at the time t. V_{w1} and V_{w2} is the independent rotational speed of the left and right wheel, respectively. V_{ovx} and V_{ovy} is the speed of the center point ov in the direction X' and Y', respectively. $x_{ov}(t)$ and $y_{ov}(t)$ is the position of the mobile robot at time t. $\omega_v(t)$ is the angular speed of the mobile robot at time t.

2.2 Kinematics model

In the global coordinate system {O, X, Y}, the constraints (pure rolling without slide) can be expressed as:

$$\dot{y}_{ov}\cos\phi - \dot{x}_{ov}\sin\phi = 0 \tag{1}$$

The kinematics model can be built:

$$\begin{bmatrix}\dot{x}_{ov}\\ \dot{y}_{ov}\\ \dot{\phi}_{ov}\end{bmatrix} = \begin{bmatrix}\cos\phi & 0\\ \sin\phi & 0\\ 0 & 1\end{bmatrix}\begin{bmatrix}v_{ov}\\ w_{ov}\end{bmatrix} \tag{2}$$

The motion equation of the two-wheeled differential drive system is described as below:

$$\begin{cases}\omega_v(t) = \dfrac{V_{w1}}{R - 1/2}\\ \omega_v(t) = \dfrac{V_{w2} - V_{w1}}{l}\end{cases}$$

(a) The developed SDLG-1

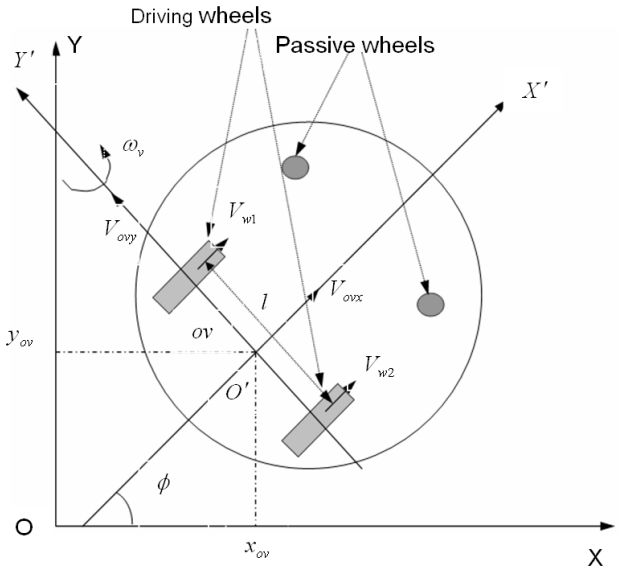

(b) Schematic diagram

FIGURE 1: The mobile robot SDLG-1

$$\begin{cases} \omega_v(t) = \dfrac{V_{w2} - V_{w1}}{l} \\ R(t) = \dfrac{l}{2} \cdot \dfrac{V_{w1} + V_{w2}}{V_{w2} - V_{w1}} \end{cases}$$
$$\begin{cases} V_{ovx} = \omega_v(t).R(t) = \frac{1}{2}.(V_{w2} + V_{w1}) \\ V_{ovy} = 0 \end{cases} \quad (3)$$

The position and orientation of the bodywork at a specific time can be indicated as:

$$\begin{cases} \phi(t) = \phi(0) + \int_0^1 \dfrac{V_{w2}(t) - V_{w1}(t)}{l} dt \\ x_{ov}(t) = x_{ov}(0) + \int_0^1 \dfrac{1}{2}(V_{w2} + V_{w1}).\cos\phi(t) dt \\ y_{ov}(t) = y_{ov}(0) + \int_0^1 \dfrac{1}{2}(V_{w2} + V_{w1}).\sin\phi(t) dt \end{cases} \quad (4)$$

Where, $v(t)$ and $\omega(t)$ is the linear speed and angular speed at time t, respectively, $x(t)$ and $y(t)$ are the position of the mobile robot at time t, which is represented by the center point ov on the drive axle. ϕ is the included angle between the robot advancing direction and the X axis. R is the turning radius.

In the control of the mobile robot, its expected motion status is tracked by working out $v(t)$ and $\omega(t)$ using control arithmetic and the speeds of two driving wheels based on the above equations. As can be known from the above motion equations, the motion system of the structure cannot make abrupt changes in motion directions. The reason it that the system can only follow the trajectory curve with continuous changes of the tangent angles when the two wheels make same direction movements. The first order derivative of its motion curve must be continuous. When the curve with the abrupt changes of the motion directions is being tracked, it is done by making rotation of the mobile robot without advancing. The occurrence of such curves should be avoided as far as possible in the path planning.

3. NAVIGATION CONTROL

A sensor ring composed of twelve sensors is installed on the robot to get the information of distance in every direction. Every sensor is used to detect the distance between the nearby objects and the robot. As is indicated in Figure 2, “0” is the front end of the robot, “6” is the back end, and the sectional drawings are the objects. What should be noted here is that the sonar wave packet has a certain effective width and the distance information of the sensors is got by calculating the wave packet which first reaches the surface of the object (the wave packet is not necessary to reach the middle distance between the sensor and the obstacle) [14-16]. In Figure 2, sonar sensor 0 and 11 has not received any echoes, so no precise calculation of the distance is possible (for which, a margin can be set).

The twelve sonar sensors are indicated as Si (i=0, 1, …, 11). The output of Si is expressed as Ri. When the angle of each sensor is set with respect to the current motion direction of the robot, the existence of obstacles in every direction of the robot and the distance between the robot and the obstacle can be determined. If Si does not detect any object in its corresponding direction, Ri = -1; if Si detects an obstacle in the direction, Ri >0. l and r are used to indicate the approximate extent of the obstacles on the right and left sides of the robot at its present position. When the obstacle on the left is closer to the robot, it turns right; when the obstacle on the right is closer, it turns left. The value of l and r can be determined as follows:

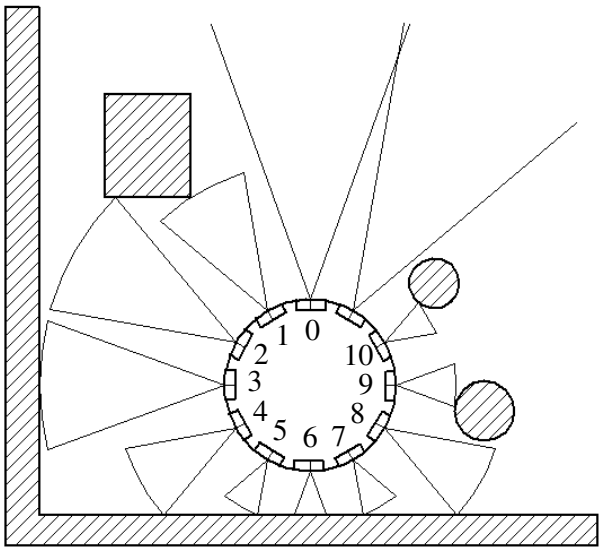

FIGURE 2: Sonar sensors and their distance finding range

$$\begin{cases} l = \sum_{1}^{4} \frac{|\cos\alpha_i|}{R_i + R_0} \\ r = \sum_{8}^{11} \frac{|\cos\alpha_i|}{R_i + R_0} \end{cases} \qquad \alpha_i = (2k+1)\frac{1}{24} * 2\pi, (k = 0,1,2...11) \tag{5}$$

Where R0 is set as a margin to prevent l and r from going as infinite. α_i is the direction angle of the i^{th} ultrasound in the partial coordinate system of the robot, and $\cos\alpha_i$ is the effect coefficient of the obstacle to the current robot that the i^{th} ultrasound detects. When the output of Si is over 0, Ri is the output of Si; when it is below 0, Ri is the detection range of the ultrasound. Suppose Imin indicates that high level behaviour does not restrain its low level behaviour, when the sensor does not detect any obstacle, avoid-obstacle behaviour will not be activated, and the biggest ultrasonic detecting range is bigger than Ri. Suppose Imax is used to judge whether the obstacle is very close to the robot, when it is quite close, the robot will stop to avoid collision. Suppose the maximum speed of the robot is $v_{\max}$, the sampling period is Δt, and the distance between the robot and any static obstacle is no less than its biggest step length $v_{\max}\Delta t$, Imin and Imax can be expressed as:

$$\begin{cases} I_{\min} = \sum_{8}^{11} \frac{|\cos\alpha_i|}{R_{range} + R_0} = \sum_{1}^{4} \frac{|\cos\alpha_i|}{R_{range} + R_0} \\ I_{\max} = \frac{1}{v_{\max}\Delta t + R_0} \end{cases} \tag{6}$$

Three behaviour modules of follow-wall, avoid-obstacle and move-to-goal form the subsumption architecture in the navigation control of the robot, as indicated in Figure 3, in which s indicates restraint. Different behaviour module determines its behaviour output according to the input of the sensor, and high-level behaviour restrains low-level behaviour. Follow-wall behaviour makes the robot free of deadlock, avoid-obstacle behaviour makes the robot avoid static obstacles in the environment, and move-to-goal behaviour makes the robot go to its goal. In this paper, the navigation method uses the above three behaviours to plan and control the input vector q:

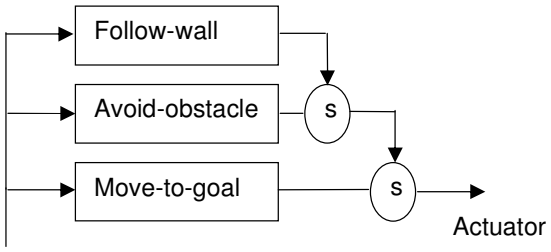

FIGURE 3: SDLG-1 control structure

3.1 Follow-wall Behaviour

After the behaviour is activated, the robot will move along the edge of the obstacle. The conditions of activation (A) of the follow-wall behaviours are:

$$\begin{aligned}&(l > I_{\max} \cap r > I_{\max}) \cup (\zeta > \pi/2 \cap R_2 > 0 \cap R_4 > 0) \\ &\cup (\zeta < -\pi/2 \cap R_8 > 0 \cap R_{10} > 0)\end{aligned} \tag{7}$$

When the target point is in the first half cycle of the robot, and no obstacle exists in the direction of S1 and S11, follow-wall behaviour will end. So the backout condition of the follow-wall behaviour (B) is :

$$\zeta \in [-\pi/2, \pi/2] \cap R_1 < 0 \cap R_{11} < 0 \tag{8}$$

Where, ζ is the angle between the current motion direction of the robot and the connecting line between the robot and the target point, which can be calculated according to the difference between the number of rolling circles of the right and left driving wheels, and the activation condition and backout condition are boolean type variables, which is true when its value is 1. The boolean type variables are defined as:

$$c = \begin{cases} 1, A = 1 \\ 0, B = 1 \end{cases} \tag{9}$$

where A and B is the activation condition and backout condition used in Equation (7), respectively.

Thus, the effective condition of follow-wall behaviour is $A \cup C$.

3.2 Avoid-Obstacle Behaviour

The effective condition of avoid-obstacle behaviour is:

$$(\bigcup_{0 \le i \le 4} R_i \cup \bigcup_{8 \le i \le 11} R_i) > 0 \cap \overline{A} \cap \overline{C} \tag{10}$$

The obstacle dead ahead of the robot has the biggest effect on it, so the output of avoid-obstacle behaviour must satisfy the demand of avoiding the obstacle. Its control input is:

$$\begin{cases} v_{a0}(t) = v_{\max} \\ \omega_{a0} = \begin{cases} \theta_{a0} / \Delta t, l \le r \\ -\theta_{a0} / \Delta t, l > r \end{cases} \end{cases} \tag{11}$$

where v_{a0} and ω_{a0} is the linear speed and rotary speed of the mobile robot for the next step, respectively, $v_{\max}$ is the maximum linear speed, θ_{a0} is a set of values, indicating the orientation of the robot in its one-step turn.

3.3 Move-to-Goal Behaviour

The effective condition of move-to-goal behaviour is:

$$\bigcap_{0\le i\le 4} R_i \cap \bigcap_{8\le i\le 11} R_i = -1 \tag{12}$$

When the robot does not detect any obstacle, move-to-goal behaviour is activated. A polar coordinate is established with the starting point S as the Pole point, X axis as the pole axis, as is indicated in Figure 4, the current position of the robot R is:

$$(\rho_R, \beta(t), 0 \le \beta(t) \le 2\pi \tag{13}$$

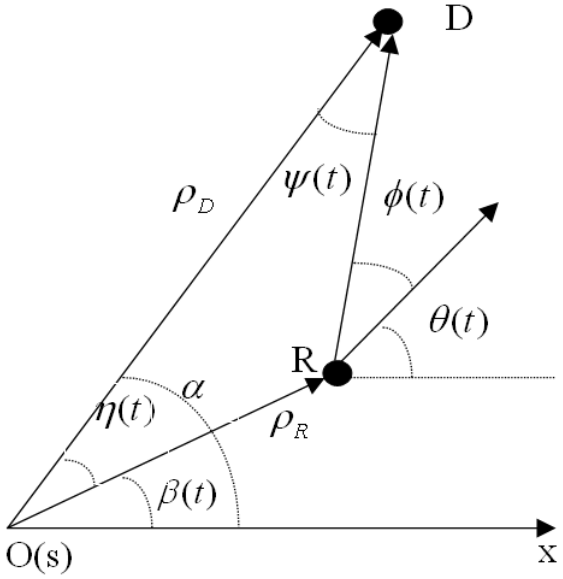

FIGURE 4: Polar coordinate of the move-to-goal behaviour

The coordinate of the goal point D is:

$$(\rho_D, \alpha), 0 \le \alpha \le 2\pi \tag{14}$$

The distance between the current position and the goal point is $\left|\overrightarrow{RD}\right|$ and the expected turning angle is $\phi(t)$. Because of the limit of the maximum angular rate $\omega_{\max}$, the planned control input of move-to-goal behaviour is:

$$v_{mtg}(t) = \begin{cases} v_{\max}, \left|\overrightarrow{RD}\right| \ge v_{\max}\Delta t \\ \left|\overrightarrow{RD}\right| / \Delta t, \left|\overrightarrow{RD}\right| < v_{\max}\Delta t \end{cases} \tag{15}$$

where $v_{\max}$ is the maximum straight-line motion speed of the robot, and also:

$$\omega_{mtg}(t) = \begin{cases} \omega_{\max}, \omega_\tau(t) \ge \omega_{\max} \\ \omega_\tau(t), \omega_\tau(t) \le \omega_{\max} \end{cases} \tag{16}$$

Where, $\omega_\tau(t) = \gamma(t) / \Delta t$

$$\gamma(t) = \begin{cases} \delta(t), \delta(t) \in [0, 2\pi] \\ \delta(t) + 2\pi, \delta(t) \in [-2\pi, 0] \\ \delta(t) + 4\pi, \delta(t) \in [-3\pi, -2\pi] \\ \delta(t) - 2\pi, \delta(t) \in [2\pi, 3\pi] \end{cases} \tag{17}$$

Where, $\delta(t) = (-1)^k \psi(t) + \alpha - \theta(t)$

$$k = \begin{cases} 0, \alpha - \beta(t) \in [0, \pi] \cup [-2\pi, \pi] \\ 1, \alpha - \beta(t) \in [-\pi, 0] \cup [\pi, 2\pi] \end{cases} \tag{18}$$

$$\psi(t) = \arccos \frac{\rho_D - \rho_R \cos\eta(t)}{\sqrt{\rho_D{}^2 + \rho_R{}^2 - 2\rho_D\rho_R \cos\eta(t)}} \tag{19}$$

$$\eta(t) = \begin{cases} \alpha - \beta(t), \alpha - \beta(t) \in [0, \pi] \\ \beta(t) - \alpha, \alpha - \beta(t) \in [\pi, 0] \\ \beta(t) - \alpha + 2\pi, \alpha - \beta(t) \in [\pi, 2\pi] \\ \alpha - \beta(t) + 2\pi, \alpha - \beta(t) \in [-2\pi, -\pi] \end{cases} \tag{19}$$

According to the above equations, the robot can plan a relatively good path without collision in complicated environment. The above-discussed three navigation behaviours have good stability.

4. SIMULATION EVALUATION

Experiment I: The environment of obstacle avoidance simulation experiment is a section of corridor in the simulation lab environment, as is shown in Figure 5, where the red colour shows the walls and the blue colour shows the obstacles. A distance of 8 meters is set between the starting point S and the object point G and 4 static obstacles are placed between the two points. The corridor is 3 meters wide. The width of obstacles 1 and 2 is 0.3 meter. The horizontal distance between obstacle 1 and 2 is 1.2 meters. The distance between obstacle 2 and 3 is 0.8 meter. The distance between obstacle 3 and 4 is 0.9 meter. Obstacle 3 is an irregular object, and obstacle 4 is a ball with a diameter of 0.7 meter. The diameter of the robot is 0.45 meter.

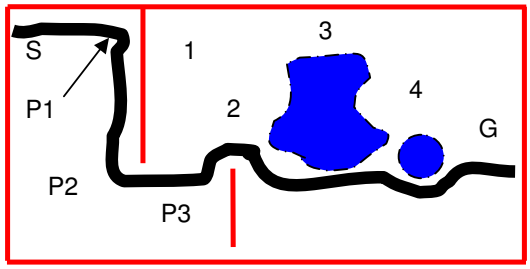

FIGURE 5: Simulation of the autonomous obstacle avoidance

The robot first entered into the follow-wall behaviour. When it reached the point P1, it detected obstacle 1. Because the wall and obstacle 1 form a turn, the robot will sway from side to side and enter into the “canyon effect”, one of the possible solutions is to add states in programmes so that the robot can use them to memorize the action that it is taking at present and consequently to prevent itself from making opposite operation to make itself sway from side to side. Then it continued its follow-way behaviour. It made forward-right movement to evade obstacle 1. When it reached the point of P2, navigation behaviour was activated again. Between the position of P2 and the position of P3, the follow-wall behaviour and made by the robot switched frequently. When the robot detected obstacle 3 and obstacle 4, the obstacle avoidance behaviour was activated, and finally it reached object G. Figure 5 shows the simulated path of the mobile robot. The simulation results show this behaviour-based navigation can activate corresponding behaviours according to the environment. The three behaviours collaborate each other closely and consequently avoid the four drawbacks by using the PFM. So the behaviour-based navigation introduced in this paper is more concise and more convenient for realization than that of PFM.

Experiment II: In the experimental fied with traps, the robot navigated by traditional potential field method cannot escape from the traps as shown in Fig. 6. As shown in Fig. 7, by the new navigation method, the robot escapes from the trap quickly. The robot can escape from the trap clockwisely or counterclockwisely denpending on the programming parameters. Further hardware and software realization are needed for the automatic direction selection to realize the shortest moving path.

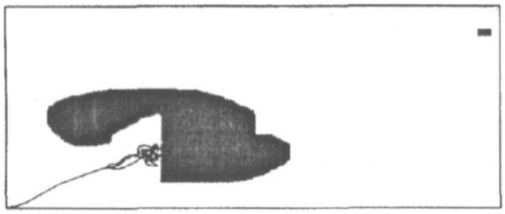

FIGURE 6: Results by traditional potential Field method

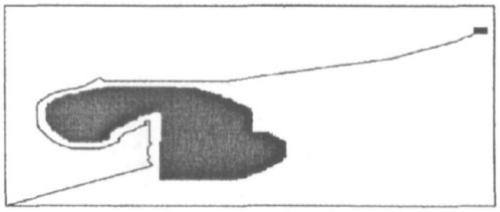

FIGURE 7: Results by the proposed navigation method

5. CANYON EFFECT AND COUNTERMEASURES

If there are a lot of obstacles or some obstacles have concave geometries in the environment, the avoid-obstacle behaviour may fail. As shown in Figure 8, such mistakes may happen at the sharp corner of the obstacle. Under such circumferences, the robot will turn to right due to the detection of obstacle at the left side. But it will turn back to left due to the detection of obstacles at the right side. Consequently, the robot changes its directions endlessly. This phenomena is the so-called canyon effect. In order to avoid such effects, states are added to the strategy as shown in Figure 9.

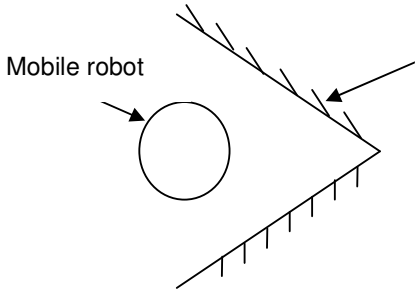

FIGURE 8: Canyon effect

In Figure 9, Text-timer(X) is the timing function always feedback true state. X is R or L representing the right or left drive wheel. Function Start-timer (X,T) is to create a timer for X and T is the timing time. Rotation and Translation is the rotating speed and translating speed of the robot, respectively.

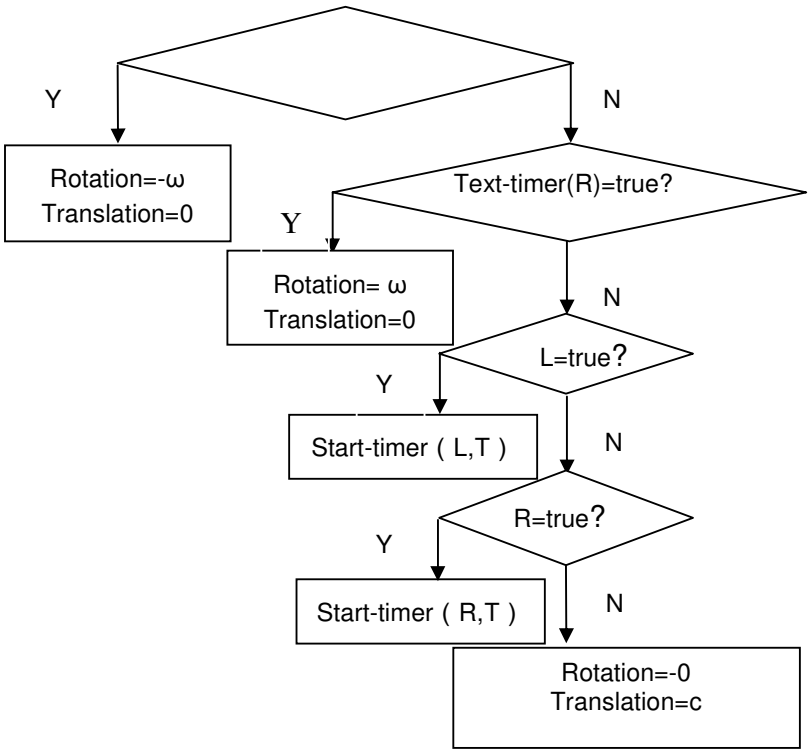

FIGURE 9: Diagram for eliminating the canyon effects

6. EXPERIMENTAL EVALUATIONS

Based on the coordinate setting as shown in Figure 1, the position of point O' under coordinate ΣO is represented by the vector P=[x y Φ]T. Φ is the orientation of the mobile robot.Given the arc path as: x=2cos(Φ), y=2sin(Φ), and Φ=0.03t, based on the navigation strategy mentioned above, the experimental results are shown in Figure 10.

From Figure 10 and Figure 11, the mobile robot SDLG-1 has realized navigations fro expected paths, which validated the navigation strategies introduced in the paper.

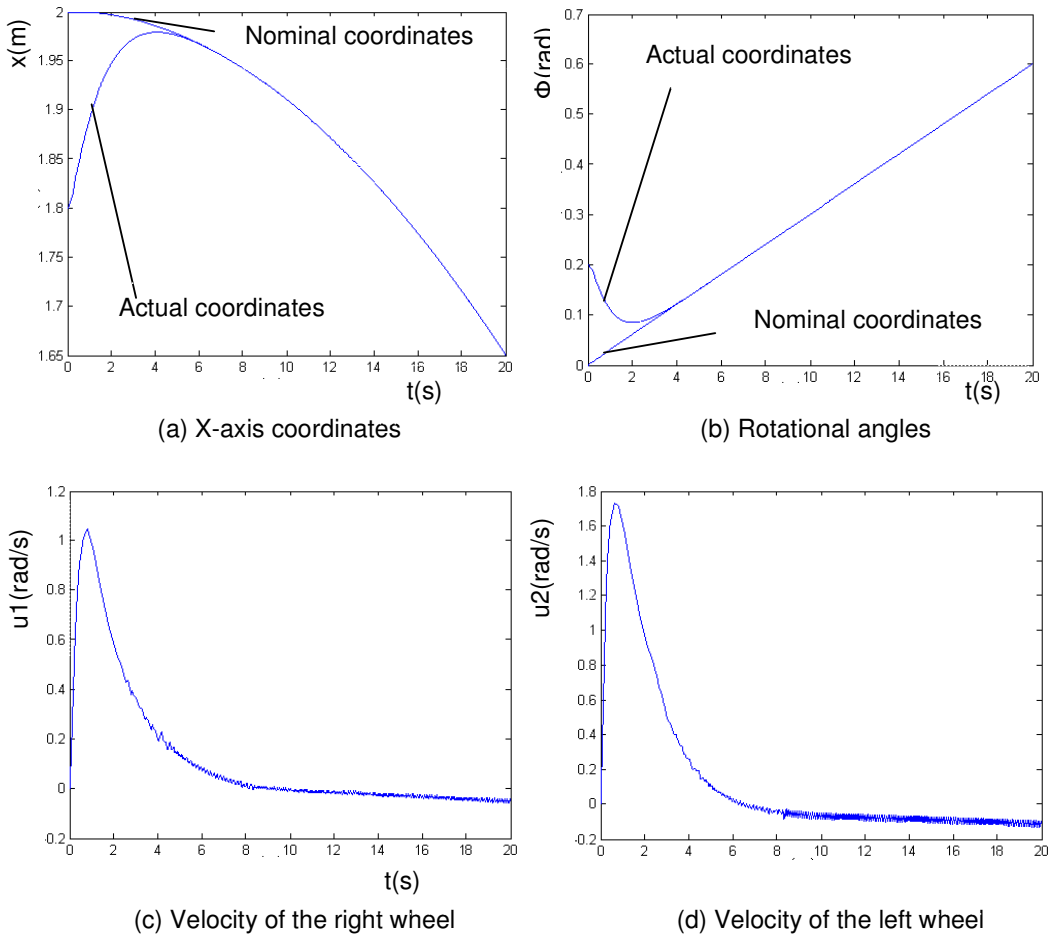

(a) X-axis coordinates

(b) Rotational angles

(c) Velocity of the right wheel

(d) Velocity of the left wheel

FIGURE 10: Navigation results for arcs

7. CONCLUSION

In this paper, aiming at navigating a mobile robot, the kinematics mode is built and the behaviour-based navigation control algorithm in deducted. Totally twelve sonar sensors are used for the navigation. Compared to potential field method, the navigation strategy introduced in this paper is convenient and effective. The evaluation simulation and experiments successfully demonstrated the proposed behaviour-based navigation strategy.

8. REFERENCES

1. D.R. Parhi, M.K. Singh, "*Intelligent fuzzy interface technique for the control of an autonomous mobile robot*," Proc. IMechE Vol. 222 Part C: J. Mechanical Engineering Science, 2008, 2281-2292.

2. J. R., Andrews, N., Hogan, '*Impedance control as a framework for implementing obstacle avoidance in a manipulator, Control of Manufacturing Process and Robotic Systems,"* ASME, Boston, 1983, 343-351.

3. O., Khatib, "*Real-time obstacle avoidance for manipulators and mobile robots*," IEEE International Conference on Robotics and Automation, St. Louis, Missouri, 1990, 500-505.

4. Y. Koren, J. Borenstein," *Potential field methods and their inherent limitations for mibilt robot navigation*," Proceedings of the IEEE Conference on Robotics and Automation, Sacramento, California, 1991, 1398-1404.

5. C. Thorpe, A. Stentz, S. Shafer, "*An architecture for autonomous vehicle navigation,"* Computers in Aerospace Conference, 5th Long Beack, CA, 1985, 22-27

6. B.H. Krogh, C. Thorpe, "*Integrated path planning and dynamics steering control for autonomous vehicles,"* Proceedings of the 1986 IEEE International Conference on Robotics and Automation, SFO, California, 1986, 1664-1669.

7. R.A. Brooks, "*A robust layered control system for a mobile robot,"* IEEE Journal of Robotics and Automation, Vlo.RA-2, 1986, 14-23.

8. R.C. Arkin, "*Motor schema-based mobile robot navigation"*, The International Journal of Robotics Research, 1989, 92-112.

9. J. Borenstein, Y. Koren, "*Real-time obstacle avoidance for fast mobile robots",* IEEE Transactions on Systems, Man, and Cybernetics, 1989, 1179-1187.

10. P. Coelho, U. Nunes, "*Path-following control of mobile robots in presence of uncertainties,*"IEEE Transactions Robotics, 2005, 21:252-261.

11. G. Antonelli, S. Chiaverini, G. Fusco, "*A calibration method for odometry of mobile robots based on the least-squares technique"*: Theory and experimental validation, 2005, 21:994-1004.

12. J.M.M. Tur, J.L. Gordillo, C.A. Borja, *A closed-form expression for the uncertainty in odometry position estimate of an autonomous vehicle*, IEEE Transactions on Robotics, 2005, Vol. 21, 1017-1022.

13. Joseph L. Jones, Daniel Roth*," Robot programming: a Practical Guide to Behaviour-Based Robotics",* 2004, McGraw-Hill.

14. Hongbo Wang and takakazu Ishimatsu, "*Vision-based Navigation for an Electric Wheelchair Using Ceiling Light Landmark* ".Journal of Intelligent and Robotic Systems, 2005. 41: 283-314

15. Hongbo Wang, Chaochao Chen and Zhen Huang Ultrasonic Sensor Based Fuzzy-neural "*Control Algorithm of Obstacle Avoidance for Mobile Robot,Lecture Notes in Computer Science,Springer-Verlag Berlin Heidelberg"*, 4491(1): 824–833

16. Hongbo Wang, Ke Yu and Hongnian Yu, "*Mobile Robot Localisation Using ZigBee Wireless Sensor Networks and a Vision Sensor"*, International Journal of Modelling, Identification and Control,10(3/4):184-193,2010.